Role of copper homeostasis in the pathogenesis of

Streptococcus pyogenes

Tina Hong Dao

Biochemistry and Molecular Biology
Rhodes College
Memphis, Tennessee

2015

This Honors paper by Tina H. Dao has been read and approved for Honors in

Biochemistry and Molecular Biology.

Dr. Loretta Jackson-Hayes

Dr. Jonathan FitzGerald

Dr. Terry W. Hill

I give permission for public access to my Honors paper and for any copying or digitization to be done at the discretion of the College Archivist and/or the College Librarian.

Signed_____

      Tina H. Dao

Date: May 1, 2015

Acknowledgments

I would like to express my deep gratitude to all members of the Rosch laboratory, specifically my mentors Dr. Jason Rosch and Dr. Michael Johnson for their guidance and support throughout my research experience at St. Jude's Children's Research Hospital.

I would also like to give special thanks to my honors thesis committee members Dr. Loretta Jackson-Hayes, Dr. Jonathan FitzGerald, and Dr. Terry Hill for their advice, support, and critical review of my honors research paper.

CONTENTS

List of Figures and Tables

Role of copper homeostasis in the pathogenesis of

Streptococcus pyogenes

ABSTRACT

Metals serve as cofactors of many crucial proteins in various cellular processes. Copper, in particular, not only is an essential trace element found in all eukaryotes and some prokaryotes, but it also has antimicrobial properties. The mammalian host exploits copper's antimicrobial properties to kill bacteria during the innate immune response. Copper efflux mechanisms have been highly conserved in bacterial systems to minimize toxicity. Previous studies have shown that deletion of the copper exporter gene *copA* in *Streptococcus pneumoniae* resulted in hypersensitivity to elevated intracellular copper. *Streptoccocus pneumoniae* and *Streptococcus pyogenes* share many similarities such as the ability to cause pneumonia and bacteremia and lyse blood cells. Currently, there are no published studies on the role of the copper efflux pump and the mechanism of copper-mediated toxicity in *S. pyogenes*. In this study, an in-frame deletion in *copA* (*SPy_1715*) was constructed in the *S. pyogenes* HSC5 wild-type strain. This mutant, named Δ*copA*, universally showed increased sensitivity to copper compared to the wild type. Virulence of the Δ*copA* mutant was attenuated. The mutant developed significantly smaller lesions 24- and 48-hours post-infection in SKH1 hairless mice. The upregulation of *czcD*, which encodes a zinc exporter, under copper stress suggests that there is crosstalk between the copper and zinc efflux systems. Data presented here on the role of the *S. pyogenes* copper efflux system in virulence and metal homeostasis will be beneficial in developing future therapeutic strategies to reduce streptococcal infections.

INTRODUCTION

   Streptococcus pyogenes is a highly prevalent human pathogen that can cause mild to severe group A streptococcal (GAS) infections, such as pharyngitis, tonsillitis, otitis, necrotizing fasciitis, meningitis, and sepsis. Globally, there are 616 million cases of GAS pharyngitis and 517,000 deaths each year due to severe GAS infections (Carapetis *et al.*, 2005). According to the Centers for Disease Control and Prevention report published in 2008, 9,000 to 11,500 cases result from invasive GAS diseases each year in the United States causing 1,000 to 1,800 deaths; 6% to 7% of those cases are necrotizing fasciitis. Although penicillin is currently the most effective treatment of *S. pyogenes* infections, cases of *S. pyogenes* pharyngitis resistant to antibiotics including penicillin have been reported (Ogawa *et al.,* 2011). Therefore, potential antibiotic resistance in *S. pyogenes* necessitates development of non-antibiotic antimicrobial agents.

   Metals serve as cofactors of more than 30% of all proteins involved in cellular activities (Palm-Espling, 2012). Bacteria sequester necessary metals, such as magnesium, calcium, iron, manganese, and copper, while the mammalian host reacquires those metals and targets the bacteria with toxic metals, such as copper and zinc. A high concentration of intracellular copper is toxic to bacterial cells by inducing oxidative stress (Festa and Thiele, 2012). Nearly all bacteria have developed mechanisms to tightly regulate the influx and efflux of metals. This allows the bacteria to maintain homeostasis and circumvent the host's defense mechanism (Fig. 1A).

   There are limited data on mechanisms of copper toxicity. Recently, copper has been shown to inhibit the aerobic nucleotide synthesis pathway and iron sulfur cluster formation in *S. pneumoniae* (Johnson *et al.,* 2015a) and *E. coli* (Imlay and Macomber,

2009), respectively. However, the mechanism of copper homeostasis in *S. pyogenes* is not well understood.

In this study, function of the *S. pyogenes copA* gene (*SPy_1715)*, which is homologous to *Streptococcus pneumoniae copA* (*SP_0729)*, in the mechanism of copper toxicity and homeostasis was examined. According to the proposed mechanism of copper homeostasis in *S. pneumoniae*, as copper enters the cell, it binds to and inactivates the cop operon repressor CopY, increasing the expression of *copA* (Johnson *et al.,* 2015). Additionally, in *S. pneumoniae,* deletion of CopA decreased virulence (Johnson *et al.,* 2015b). CopA in *S. pyogenes* was predicted to export copper, which probably inhibits either the anaerobic dNTP synthesis or the duplicated aerobic dNTP synthesis (Fig. 1B). Deletion of *copA* would attenuate efflux ability and virulence of *S. pyogenes* by lowering its resistance to copper.

RESULTS

_SPy_1715,_ a _copA_ homologue that encodes the copper exporter protein CopA, is required for copper resistance in _S. pyogenes_

CopA is highly conserved among human pathogens such as _Staphylococcus aureus, S. pneumoniae,_ and _S. pyogenes._ The universally conserved copper resistance system in streptococci contains a regulator to control expression, a copper-binding protein, and a P-type ATPase, which is an exporter to mediate efflux (Rae _et al.,_ 1999). Based on sequence homology, _SPy_1715_ in _S. pyogenes_ was predicted to serve a similar function to _SP_0729,_ which exports excess intracellular copper in _S. pneumoniae._ There are several conserved regions found in both _SPy_1715_ and _SP_0729_ (Fig. 2A). _SPy_1715,_ named as _copA,_ encodes an ATPase containing a phosphatase domain TGE (295-277), a Phosphorylation Domain DKGT (423-427), a P-type ATP Binding Domain GDGIDN (620-625), and a Consensus Copper I Binding Domain CXC (379-381) (Fig. 2B). Therefore, the _copA_ gene was expected to encode a copper exporter in _S. pyogenes._

To determine the function of the _copA_ gene (_SPY_1715_) in _S. pyogenes,_ an in-frame deletion of _copA_ was constructed in the HSC5 (wild-type) strain (Fig. 3). Based on the hourly and overnight growth curves, the Δ_copA_ mutant was hypersensitive to high concentrations of copper ranging from 50 μM to 1 mM compared to the wild type and the wild-type revertant ($p \leq 0.01$) (Fig. 4A, B). In addition to growth curves, colony-forming units (CFU) of the wild type and Δ_copA_ mutant were determined. The Δ_copA_ mutant's CFUs were 2-orders of magnitude lower than the wild type and the revertant after 7 hours in 50 μM copper (Fig. 4C). Furthermore, the zone of inhibition of the Δ_copA_ mutant was larger than that of the wild type and the revertant, roughly 0.8 cm as opposed to 0.5 cm (p

≤ 0.01) (Fig. 4D). These results suggest that CopA plays a primary role as a copper

exporter in *S. pyogenes* under physiological conditions.

Virulence of the Δ*copA* mutant was highly attenuated *in vivo*

Previous studies indicated that CopA is necessary for *S. pyogenes* survival under

copper toxicity *in vitro*. Whether CopA affects *S. pyogenes* ability to infect the

mammalian host was examined in a hairless mouse model. Seven-week old, hairless mice

(SKH1) were subcutaneously infected with the wild type and the Δ*copA* mutant, and

lesion areas were measured (Fig. 5A). The Δ*copA* mutant created significantly smaller

lesions than the wild type or revertant after 24 and 48 hours ($p \leq 0.05$) (Fig. 5B, C).

Additionally, there were approximately 1-log fewer CFUs/mg/ml of the Δ*copA* mutant

than those of HSC5 or the revertant after 48 hours (Fig. 5C).

Copper toxicity increased under anaerobic conditions

The effects of copper toxicity on both the wild type and the mutant under

anaerobic conditions were studied to determine whether there was a difference in growth

between the anaerobic and aerobic conditions. In an aerobic environment simulated by

shaking incubation, both the wild type and the Δ*copA* mutant were more tolerant of

copper than under normal anaerobic conditions (Fig. 6A, B). To simulate an anaerobic

environment, ThyB pH 6.5 was supplemented with oxyrase, which removes O_2 by

combining it with H^+, and/or 100 μM $CuSO_4$ (Wiggs *et al.,* 2000). Addition of oxyrase

rendered both the wild type and the Δ*copA* mutant hypersensitive to copper, indicating

that excess copper in *S. pyogenes* becomes more toxic to growth under anaerobic conditions (Fig. 6B).

Excess copper decreases H_2O_2 production in the wild-type *S. pyogenes* and the $\Delta copA$ mutant while increasing H_2O_2 toxicity

In order to survive and continue to invade the host, *S. pyogenes* must cope with oxidative damage resulting from H_2O_2, which is a toxic substance produced by cellular metabolic processes (King *et al.,* 2000). If copper stress interferes with the protective mechanism against oxidative damage, there would be a significant reduction in survival under both copper and oxidative stress due to the $\Delta copA$ mutant's inability to export copper. In order to determine how wild-type *S. pyogenes* and the $\Delta copA$ mutant respond to oxidative stress exerted by H_2O_2 combined with copper stress, both strains were exposed to the final concentration of 0.1% H_2O_2. Although they both showed susceptibility to H_2O_2 stress, the $\Delta copA$ mutant was more susceptible to H_2O_2 than the wild type (Fig. 7A).

S. pyogenes not only regulates its response to oxidative stress from H_2O_2 but it also produces H_2O_2 under aerobic conditions (Kietzman and Caparon, 2010). Upon entry into the cell, Cu^{2+} must be reduced to Cu^+ in order to be exported. H_2O_2 produced by *S. pyogenes* can react with Cu^+ ions to produce highly reactive hydroxyl radical via Fenton chemistry, causing cellular damage or death. To determine how copper stress affects *S. pyogenes* H_2O_2 production, both strains were grown under aerobic conditions to collect H_2O_2 produced. Both the wild type and the mutant significantly reduced their H_2O_2 production by 50% and 33%, respectively, under copper stress (Fig. 7B).

The wild type HSC5 and the Δ*copA* mutant were equally sensitive to hydroxyurea

Because the Δ*copA* mutant could not tolerate high concentrations of copper, the mechanism of copper toxicity regarding cellular damage in *S. pyogenes* was investigated. Copper toxicity disrupts the aerobic nucleotide synthesis in *S. pneumoniae* by disrupting NrdF, the aerobic ribonucleotide reductase (Johnson *et al*., 2015). NrdF is a metal binding protein that can coordinate either two manganese ions, one manganese ion and one iron ion, or two iron ions (Martin and Imlay, 2011). Copper has previously been shown to displace manganese from proteins' active sites and is hypothesized to have a similar effect on NrdF (Batinic-Haberle, 1997). In addition to the aerobic nucleotide synthesis pathway found in *S. pneumoniae*, *S. pyogenes* has a distinctly different redundant pathway as *S. pyogenes* contains both NrdF1 and NrdF2. NrdF2 in *S. pyogenes* is almost identical to NrdF in *S. pneumoniae*. NrdF was predicted to bind manganese; however, NrdF1 was not predicted to bind manganese or iron and has little homology to other ribonucleotide reductases.

Even though the full contribution of the redundant pathway is not well understood, the mechanism was still expected to be conserved in both *S. pyogenes* and *S. pneumoniae*. Hydroxyurea (HU) inactivates the ribonucleotide reductase NrdF, thereby disrupting DNA synthesis, preventing DNA repair, and causing cell death (Yarbro, 1992). The pathway was chemically inhibited by 100 mM hydroxyurea under aerobic, anaerobic, and/or with copper stress. HU inhibited growth of HSC5 and the Δ*copA* mutant equally with or without sub-lethal copper stress at 100 µM under aerobic conditions (Fig. 8A). Thus, the pathway redundancy likely circumvents the HU stress. Furthermore, HU had no effect on growth of either strain under anaerobic conditions,

likely due to these bacteria using the anaerobic nucleotide synthesis pathway. However, the Δ*copA* mutant's growth was reduced in the presence of $CuSO_4$ as previously observed (Fig. 8A).

Manganese increased bacterial growth under normal aerobic conditions and also rescued *S. pneumoniae* growth under copper stress (Johnson *et al*., 2015). Thus, *S. pyogenes* NrdF2 would also serve as a manganese-dependent ribonucleotide reductase in *S. pyogenes*. The effect of manganese on *S. pyogenes* growth was examined under copper stress. Interestingly, manganese did not rescue growth performance of either the wild type or the Δ*copA* mutant. The addition of 250 µM manganese did not generate a significant increase in growth of the wild type or the Δ*copA* mutant under the copper sub-lethal concentrations of 500 µM and 100 µM, respectively (Fig. 8C). Like manganese, the addition of iron could not induce a significant increase in bacterial growth under copper toxicity (data not shown).

In addition to the Cop operon, *czcD* was upregulated under copper stress

The transcriptional profile of the *S. pyogenes* genome was examined in order to elucidate the mechanism of copper toxicity. Based on the microarray data, metal exporters showed the most notable increase or decrease in gene expression. Under copper stress, the putative copper chaperone *copZ*, the putative copper-transporting ATP-ase *copA*, and the putative negative transcriptional regulator *copY* were upregulated, roughly 3.5 to 5-fold. Interestingly, the putative zinc-efflux system membrane protein, CzcD*,* also had a 4-fold increase in expression (Table 1). The upregulation of *czcD* was confirmed

via RT-PCR. There was a 2-fold increase in *czcD* expression in the wild type and the

Δ*copA* mutant in the presence of copper (Fig. 9).

CzcD is required for zinc resistance in *S. pyogenes*

 The upregulation of *czcD* might indicate that there is a crosstalk between copper

and zinc efflux systems. To confirm its putative function as a zinc exporter, an in-frame

deletion of *czcD* was generated in *S. pyogenes.* Compared to HSC5 and the Δ*copA*

mutant, the Δ*czcD* mutant and the Δ*czcD*Δ*copA* double mutant were hypersensitive to

zinc stress. HSC5 growth without Zn^{2+} was normalized to 1. The normalized overnight

growth of the Δ*czcD* and the Δ*copA*Δ*czcD* double mutant was decreased to 80% and

60%, respectively, with 500 µM of Zn^{2+} (Fig. 10).

Compared to HSC5, the Δ*copA* mutant showed an increased sensitivity to copper stress due to depletion of intracellular zinc pools

 As the increase of zinc seemed to have a significant, but ultimately not

biologically relevant effect on the mutant, the depletion of zinc was examined. To

determine whether depletion of intracellular zinc is an underlying mechanism of copper

toxicity in *S. pyogenes,* TPEN was added to the media as a cell-permeable zinc chelator.

Both the wild type HSC5's and the Δ*copA* mutant's growth was inhibited by 100 µM

TPEN. Both strains were rescued by addition of 100 µM $ZnCl_2$. Only the wild type was

completely rescued by addition of 100 µM $CuSO_4$. The Δ*copA* mutant's growth

inhibition by TPEN was partially restored in the presence of $CuSO_4$. The mutant was

more sensitive to 100 µM $CuSO_4$ with TPEN than to 100 µM $CuSO_4$ alone (Fig. 11A).

Bacterial counts were also determined after 24 hours. Generally, the number of CFUs/ml was consistent with bacterial growth measured by optical density in each condition. However, the number of CFUs/ml of HSC5 showed a 2 to 3-log reduction under copper stress, compared to only 0.15 reduction in bacterial growth measured by OD (Fig. 11B). Addition of other divalent cations, catalase, essential amino acids, and carbohydrates could not rescue HSC5 from copper toxicity during stationary phase (Fig. 12).

DISCUSSION

In this study, the ΔcopA mutant was generated via in-frame deletion to determine the function of CopA in *S. pyogenes* survival and virulence (Fig. 3). The ΔcopA mutant became hypersensitive to copper stress due to its inability to export excess copper (Fig. 4). Based on the copper sensitivity assays, CopA is essential for copper resistance in *S. pyogenes*. There was a considerable reduction in the wild type's CFUs after 24-hour incubation with copper (Fig. 11B). The cells were intact when viewed under the microscope. These results suggest that as *S. pyogenes* enters the quiescent state, some pathways regulated during the stationary phase are targeted by copper. The identities of the pathways still remain unknown. Divalent cations would rescue the wild type if depletion of those cations were responsible. H_2O_2 produced would be converted into H_2O and O_2 by catalase. If the biosynthesis of amino acids and carbohydrates were inhibited, supplementing the amino acids and carbohydrates would restore growth. However, addition of many different components could not rescue HSC5 from copper toxicity during stationary phase (Fig. 12). This demonstrates that depletion of divalent cations, accumulation of H_2O_2 in the media, and inhibition of biosynthetic and metabolic pathways are not the underlying causes of the reduction in survival after stationary phase.

It was previously hypothesized that the mechanism of copper toxicity is via free radical production in conjunction with H_2O_2, which *S. pyogenes* produces under aerobic conditions. However, experimental data showed that copper toxicity became more detrimental to both the wild type and the ΔcopA mutant as the growing conditions changed from aerobic to anaerobic (Fig. 6).

To survive in the host's environment, *S. pyogenes* must have developed mechanisms against oxidative damage caused by H_2O_2. It utilizes PerR as an oxidative stress-responsive repressor to overcome H_2O_2 toxicity (Ricci *et al.,* 2002). When both the wild type and the $\Delta copA$ mutant were exposed to H_2O_2, the $\Delta copA$ mutant was more susceptible to H_2O_2 stress than the wild type. Both strains produced significantly less H_2O_2; however, under copper stress, the wild type reduced H_2O_2 more effectively than the mutant (Fig. 7B). In fact, *S. pyogenes* does not produce H_2O_2 until late phase growth (Seki *et al.,* 2004). Taken together, the bacteria probably turned down H_2O_2 production under copper stress. These results imply that copper might be killing the bacteria via a Fenton chemistry independent pathway. One possibility is that increased copper toxicity under anaerobic conditions could result from the reduction of Cu^{2+} to Cu^+, which is more stable in anaerobic conditions and can be more reactive (McBrien, 1980).

In vitro, the $\Delta copA$ mutant was hypersensitive to H_2O_2 stress. *In vivo*, when exposed to H_2O_2 produced by the host's cellular processes, it created smaller lesions in the hairless mouse model. Lesion size and bacterial counts show how invasive the bacteria are in the host. Thus, the mutant was highly attenuated *in vivo* compared to the wild type (Fig. 5). The attenuation of the $\Delta copA$ mutant suggests that CopA is necessary for *S. pyogenes* virulence.

To elucidate the mechanism of copper toxicity to *S. pyogenes* without introducing lethal mutations*,* the aerobic nucleotide synthesis pathway was chemically inhibited by hydroxyurea (HU). Interestingly, HU did not affect the wild type and the mutant's growth under anaerobic conditions, showing that *S. pyogenes* was unable to alternate its anaerobic and aerobic pathways. If excess copper inhibits the aerobic pathway, then

addition of hydroxyurea would additively or synergistically reduce the growth of the Δ*copA* mutant under copper stress. However, HU killed the wild type and the Δ*copA* mutant equally with or without copper stress (Fig. 8B). In *S. pneumoniae,* highly accumulated copper targets the manganese- or iron-dependent, aerobic nucleotide synthesis pathway because manganese rescued the Δ*copA* mutant's growth (Johnson *et al.*, 2015). In contrast, neither manganese nor iron could rescue Δ*copA* mutant from copper toxicity in *S. pyogenes* (Fig. 8C). The redundant pathway does not have copper binding sites, so excess intracellular copper might not inhibit the aerobic nucleotide synthesis pathway in *S. pyogenes.* Thus, copper may be either targeting a different protein in the aerobic nucleotide synthesis pathway and/or causing toxicity through a different mechanism. This leads to the following speculations: first, although NrdF is conserved in both *S. pneumoniae* and *S. pyogenes,* it is not manganese- or iron-dependent; second, *S. pyogenes* might use non-manganese or non-iron dependent NrdE in the redundant pathway for nucleotide synthesis under aerobic conditions (Fig. 13).

A global transcriptional profile of *S. pyogenes* was analyzed to determine whether there are other possible mechanisms underlying copper toxicity. The 5-fold increase in gene expression of *copA* supports the prediction that CopA is involved in exporting excess intracellular copper. Not only *copA* but also *czcD* was upregulated with a 4-fold increase in expression under copper stress (Table 1). The Δ*czcD* mutant was hypersensitive to high zinc concentrations, indicating that CzcD is a zinc exporter responsible for maintaining zinc homeostasis (Fig. 10). These results also suggest that there is crosstalk between the copper and zinc efflux systems in *S. pyogenes*. Under copper stress, *S. pyogenes* exports excess copper to maintain copper homeostasis.

Simultaneously, it exports intracellular zinc, thereby disrupting zinc homeostasis. Since zinc is required for certain cellular activities, depletion of intracellular zinc renders *S. pyogenes* hypersensitive to TPEN and copper (Fig. 14A). Neither the wild type nor the Δ*copA* mutant could survive when intracellular zinc was chelated by TPEN. However, addition of $CuSO_4$ and $ZnCl_2$ completely rescued the wild type from TPEN toxicity (Fig. 11). TPEN has higher affinity for Cu^{2+} than for Zn^{2+} (Cu^{2+}, 3 x 10^{20} M^{-1}; Zn^{2+}, 4 x 10^{15}, and it does not chelate intracellular Cu^+ (Huyn *et al.,* 2001). As a result, in the wild type, TPEN preferentially chelated extracellular and intracellular Cu^{2+}; therefore, it was unavailable to deplete the intracellular zinc pool (Fig. 14B). The Δ*copA* mutant was hypersensitive to sub-lethal concentrations of Cu^{2+} in the presence of TPEN. As Cu^{2+} enters the cell, it is reduced to Cu^+, which is then exported by CopA present in the wild type (Fig. 14C). Without CopA, the Δ*copA* mutant could not export Cu^+. Since TPEN does not chelate Cu^+, accumulation of Cu^+ becomes toxic to the mutant (Fig. 11). These data indicate that dysregulation of zinc export possibly plays a role in mediating copper toxicity in *S. pyogenes.*

The following experiments are in progress to confirm intracellular zinc depletion as an indirect cause of copper toxicity. Previously, TPEN was used as a cell-permeable chelator of zinc and copper. DTPA is also a zinc and copper chelator, but it is cell-impermeable. It chelates only extracellular Zn^{2+} and Cu^{2+} (Cho *et al.,* 2007). If intracellular zinc depletion causes copper toxicity, then the Δ*copA* mutant would not be hypersensitive to Cu^{2+} under normal intracellular Zn^{2+} concentrations. Additionally, inductively coupled plasma mass spectrometry (ICP MS) and zinc specific fluorescent dyes are expected to show an increase in intracellular concentration of Cu^+ or a decrease

in intracellular Zn^{2+}. Samples for ICP MS were prepared and sent to our collaborator in Australia in January, and data are expected to return soon.

The next objective is to gain insights into the regulation of the zinc efflux system in conjunction with the copper efflux system in *S. pyogenes.* A zinc-dependent repressor named SczA in *Lactococcus lactis* was shown to inhibit *czcD* expression by binding to the gene's upstream operator in the absence of zinc. However, when zinc is present, SczA binds to the activating element of *czcD,* upregulating *czcD* transcription (Mu *et al.,* 2013). *S. pyogenes* also has a putative SczA (*SPy_0845)* with significant homology to *L. lactis* SczA. *S. pyogenes* SczA is predicted to serve similar functions. We expect to have SczA purified within the next month. To date, *sczA* has been inserted into the pMGSC7 plasmid, and the construct has been transformed into *E. coli* BL21 cells. The most recent two attempts at protein purification did not yield pure and concentrated protein. However, modifications in the protocol are underway, including increasing stringency of wash steps to decrease non-specific binding of other proteins, lysing cells via microfluidization, and combining His-tagged purification with size-exclusion chromatography. After SczA is purified, an electrophoretic gel mobility shift assay will be performed in order to assess the effect of copper on SczA binding to its target sequence in the *czcD* promoter. In the previous experiment, the zinc exporter gene *czcD* was upregulated under copper stress. It is hypothesized that SczA when bound to copper would not bind to the promoter of *czcD* to inhibit *czcD* expression.

METHODS

In-frame deletion of *copA*

An in-frame truncation mutant version of *copA* (*SPy_1715*), in which bases from 216 to 595 coding for the Consensus Copper I Binding domain were deleted, was cloned into a temperature-sensitive vector and electroporated into *S. pyogenes*. The truncated sequence was crossed into the chromosome via recombination when transformants were transferred to non-permissive temperature. After the truncated and full-length *copA* were both encoded on the chromosome, cells were transferred to permissive temperature inducing second recombination, which resulted in half of the cells with the full-length *copA* gene and half with the truncated version. The truncated version was then selected by PCR screening and verified by sequencing.

Growth curves

HCS5 (wild type), HSC5 Revertant, and the Δ*copA* mutant were grown overnight anaerobically at 37$^{\text{o}}$C in ThyB (30 g Todd Hewitt Broth and 2 g of Yeast Extract / 1 L of dH$_2$O). Then, 200 µL of the overnight culture at OD ranging from 0.6 to 0.8 (where the bacteria reach their log phrase) were inoculated into triplicate samples of 10 mL of ThyB pH 6.5 containing the following reagents: varying concentrations of CuSO$_4$, and/or 7.5 mM of HU, and/or 20 µL/mL oxyrase, and/or varying concentrations of MnSO$_4$, and/or 100 µM TPEN, or 500 µM ZnCl$_2$ and allowed to grow under the anaerobic conditions for hourly and overnight growth curves measured at 600 nm. Since HU becomes ineffective if left in ThyB overnight, only the 7-hour time points were analyzed.

CFU

HSC5, HSC5 revertant, and the Δ*copA* mutant after growing in ThyB containing 50 µM

CuSO$_4$ and/or 100 µM TPEN for 7 hours were serial diluted, then 100 µL were plated on

ThyB plates (30 g Todd Hewitt Broth, 14 g of Bactor Agar, and 2 g of Yeast Extract / 1 L

of dH$_2$O) overnight in order to determine colony forming units (CFU).

Zone of inhibition

For the zone of inhibition assay, 100 µL of culture OD 0.2 were plated on ThyB plates

containing a filter paper disk in the center that absorbed 10 µL of 1M CuSO$_4$. These

plates were incubated anaerobically in a gas-pak jar at 37°C for 12 hours. The distance

from the edge of the filter paper disk to the border where bacteria grew was measured as

the zone of inhibition.

Chromosomal DNA extraction

HSC5 was grown overnight in ThyB and 20 mM glycine. The bacterial pellet was

collected by centrifugation and washed in TE before being incubated with 50 mg

lysozyme for 1 hour at 37°C. After centrifugation, the pellet was frozen at -80°C,

resuspended in TE, and incubated at 65°C for 15 minutes in 0.4 ml 10% SDS and 0.5 ml

Tween 20 Lysing mix. Then, 25 µL RNase (5 mg/ml) was added before incubating the

suspension at 37°C for 30 minutes. Extraction with Phenol-CHCl$_3$ and CHCl$_3$ followed

by precipitation with 2.5 volumes of ethanol and washing with 70% ethanol.

Subcutaneous Infection of SKH1 (hairless) mice

HSC5 and the $\Delta copA$ mutant were grown in ThyB medium to reach OD 0.6. Bacteria were harvested by centrifugation, sonicated to disrupt streptococcal chains, and resuspended in PBS. Anesthetized 6-week old SKH1 mice were subcutaneously infected with 100 µL of bacterial suspension containing 2×10^7 bacteria. The infected mice were observed daily for signs of illness, and the images of the lesions were measured using ImageJ in order to determine the area within the asymptomatically irregular border of each lesion.

H_2O_2 sensitivity

HSC5 and the $\Delta copA$ mutant were grown to OD 0.4 and exposed to varying concentration of H_2O_2 and/or 200 µM copper for 30 minutes at room temperature. The triplicate samples were serially diluted and plated on ThyB plates overnight at 37°C with 5% CO_2 for determination of CFU.

H_2O_2 production

HSC5 and the $\Delta copA$ mutant were grown aerobically for 7 hours in ThyB with/without 50 µM copper. Bacterial supernatant was collected for the Amplex Red Hydrogen Peroxide / Peroxidase assay, then 50 µL Amplex Red reagent was added to 50 µL of the supernatant in each microplate well. The fluorescence was measured (excitation at 544 nm and emission detection at 590 nm).

Sample Preparation Inductively Coupled Plasma Mass Spectrometry

HSC5 was grown in ThyB pH 6.5 at 37°C until OD 0.3 before being incubated with 100 µM Cu^{2+} for 30 minutes. Bacterial pellets were collected via centrifugation at 3200 rpm for 10 minutes and incubated with 15 mL 1X PBS containing 10 mM EDTA at room temperature for 15 minutes. Pellets were then collected, incubated at 52°C overnight, and weighed.

RNA extraction

At OD 0.3, HSC5 and the Δ*copA* mutant were exposed to 100 µM of $CuSO_4$ for 30 minutes. Cells were pelleted at 5000 x g for 10 minutes. RNA was extracted using RiboPure RNA Purification kit.

Figure 1

A   B

Figure 1. **Proposed mechanisms**
A. Metal homeostasis in streptococci and **B. Copper homeostasis in** *S. pyogenes*

Figure 2

A

```
Italicized = Deleted in Gene Deletion
Bold = Conserved Residues
Bold Underlined = Conserved Motif for P-type ATPase Activity

Score          Identities              Positives           Gaps
3e-179        286/646(44%)            422/646(65%)        36/646(5%)

SPY_1715  82   QVLW-SALFTIPILYLAMGHMVGLWLPPFLQPDRYPFVYSFSQLLLTIPV-LVLNRHYYH  139
               Q   W +++FT+P++ L +G + G               V  +   L T P+ LV  + Y
SP_0729   22   QRFWITSIFTVPLVILMIGMLTG---------SISHQVMHWGTFLATTPIMLVAGKPYIQ  72

SPY_1715  140  NGFKALFKGHPNMDSLVALATSFAFAYSLYGVVEISLGRAHFVH-SLYFESVVVIITLIG  198
               + + +  K + NMD+LVAL  T  A+ ISL          A F   +YFES   IL +
SP_0729   73   SAWASFKKHNANMDTLVALGTLVAYFYSLV--------ALFAGLPVYFESAGFILFFVL  123

SPY_1715  199  LGKYFESRSKGRTSQAIQKLLSLKATVVRVWRNSQWQLLPLEEVSYDDLVLVQPGEKVSI  258
               LG   FE + +  TSQA++KLL L+A    V  +  + +PLE+V    DL+ V+PGEK+++
SP_0729   124  LGAVFEEKMRKNTSQAVEKLLDLQAKTAEVLSDDSYVQVPLEQVKVGDLIRVRPGEKIAV  183

SPY_1715  259  DGIIVEGHSSLDESFLTGESLPVEKGEKDNVFAGSLNGPGALTIKPDKLGNDTLLAQIIQ  318
               DG++VEG SS+DES +TGESLPV+K    D V  ++N  G L  +  +K+G++T+LAQI+
SP_0729   184  DGVVVEGVSSIDESMVTGESLPVDKTVGDTVIGSTINHSGTLVFRAEKVGSETVLAQIVD  243

SPY_1715  319  LVENAQENKAPIAAIADRVSGVFVPVVLVLALLTGVFWLVFMQESLRF-------SLTTA  371
               V+ AQ ++API  + D++SG+FVPVV++L  ++T   W V +++S+          SL
SP_0729   244  FVKKAQTSRAPIQDLTDKISGIFVPVVVILGIMTFWVWFVLLRDSVVVLGASFVSSLLYG  303

SPY_1715  372  IAVLVIACPCALGLATPTAIMVGTGRAAENGILFKGGDILEQAHQVDTVVFDKTGTITEG  431
               +AVL+IACPCALGLATPTA+MVGTGR+A+ G+L K G +L++  +V T+VFDKTGT+TEG
SP_0729   304  VAVLIIACPCALGLATPTAIMVGTGRSAKMGVLLKNGTVLQEIQKVQTLVFDKTGTLTEG  363

SPY_1715  432  KPSLQKLLTFSGDDHLILQEAASLEAYSQHPLGEAIVRAAQEAGYDSLPVEEFESLTGLG  491
               KP +  ++   GD+ +   AASLE   SQHPL EAIV+ A EAG +   VE F+SL G G
SP_0729   364  KPVVTDVI---GDEVEVFGLAASLEDASQHPLAEAIVKRASEAGLEFQTVENFQSLHGKG  420

SPY_1715  492  VTGQLEGRRLAIGNAALMGILGIDLS-CVQSVCAKASEKGQTLVYYAKEGQLRALFSIAD  550
               V+G++ G+++ +GNA ++     G+D+S    Q   +   ++ +T+V+ A + +++ L ++ D
SP_0729   421  VSGRINGKQVLIGNAKMLD--GMDISNTYQDKIEELEKEAKTVVFLAVDNEIKGLIALQD  478

SPY_1715  551  AVKEDSQATVEALHQLGIHTIMLTGDHDATAKAIASQVGITDVISQVLPDQKAGVIADLR  610
               KE+++  +  L + G+ T+MLTGD+   A+AIA Q+GI +VI+ VLP++KA  I  L+
SP_0729   479  IPKENAKLAISQLKKRGLRTVMLTGDNAGVARAIADQIGIEEVIAGVLPEEKAHEIHKLQ  538

SPY_1715  611  SQGRKVAMVGDGINDAPALAVADIGIAMGSGTDIAIESADVIIMKPDMLDLVKAMSLSRV  670
               G KVA VGDGINDAPAL+VAD+GIAMG+G+DIAIESAD++L    ++L +V+A  +S+
SP_0729   539  QSG-KVAFVGDGINDAPALSVADVGIAMGAGTDIAIESADLVLTTNNLLGVVRAFDMSKK  597

SPY_1715  671  TMRIVKENLFWAFIYNVLMIPVAMGLLHLFGGPLLNPMLAGFAMSF  716
               T   +  NLFWAFIYNV+ IP+A G+       G LNP LAG AM+F
SP_0729   598  TFHRILLNLFWAFTYNVVGIPIAAGVFSGV-GIALNPELAGLAMAF  642
```
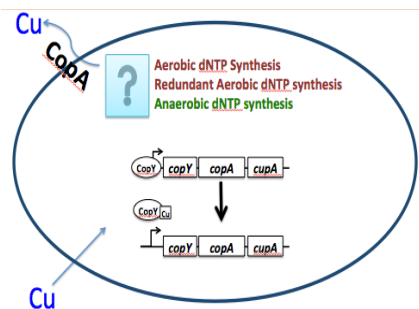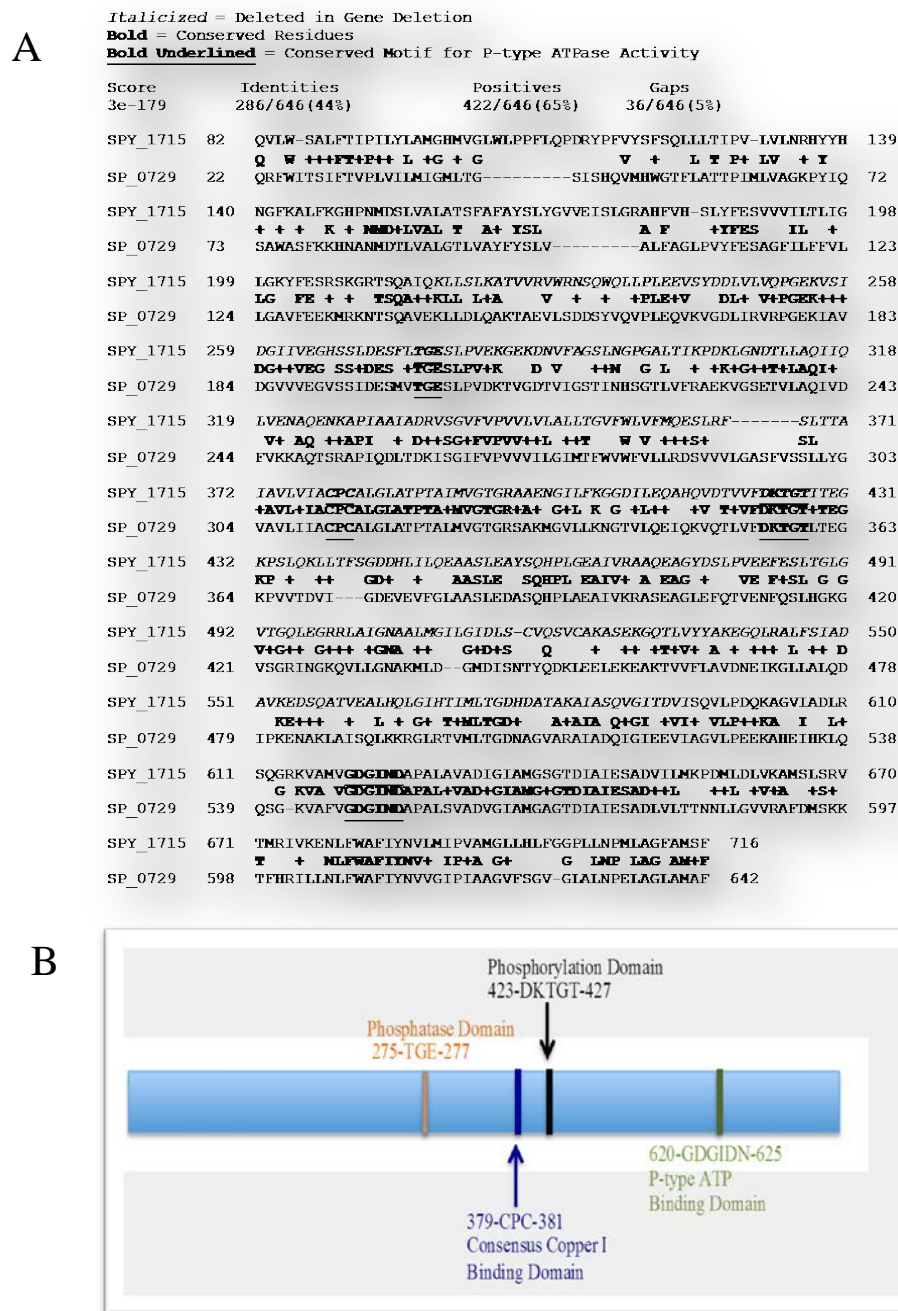
B

Figure 2. **Prediction of CopA structure and function in** *S. pyogenes* **using bioinformatics A. Protein sequence alignment of** *S. pneumoniae copA* **(***SP_0729***) and** *S. pyogenes* **copper exporter protein** *copA* **(***SPy_1715).* The sequences were aligned with NIH BLAST (http://blast.ncbi.nlm.nih.gov/Blast.cgi). The conserved features of ATPases were highlighted. **B. Schematic diagram of CopA domains.** The highlighted regions show the the protein motif conserved in *S. pneumoniae* and *S. pyogenes* CopA.
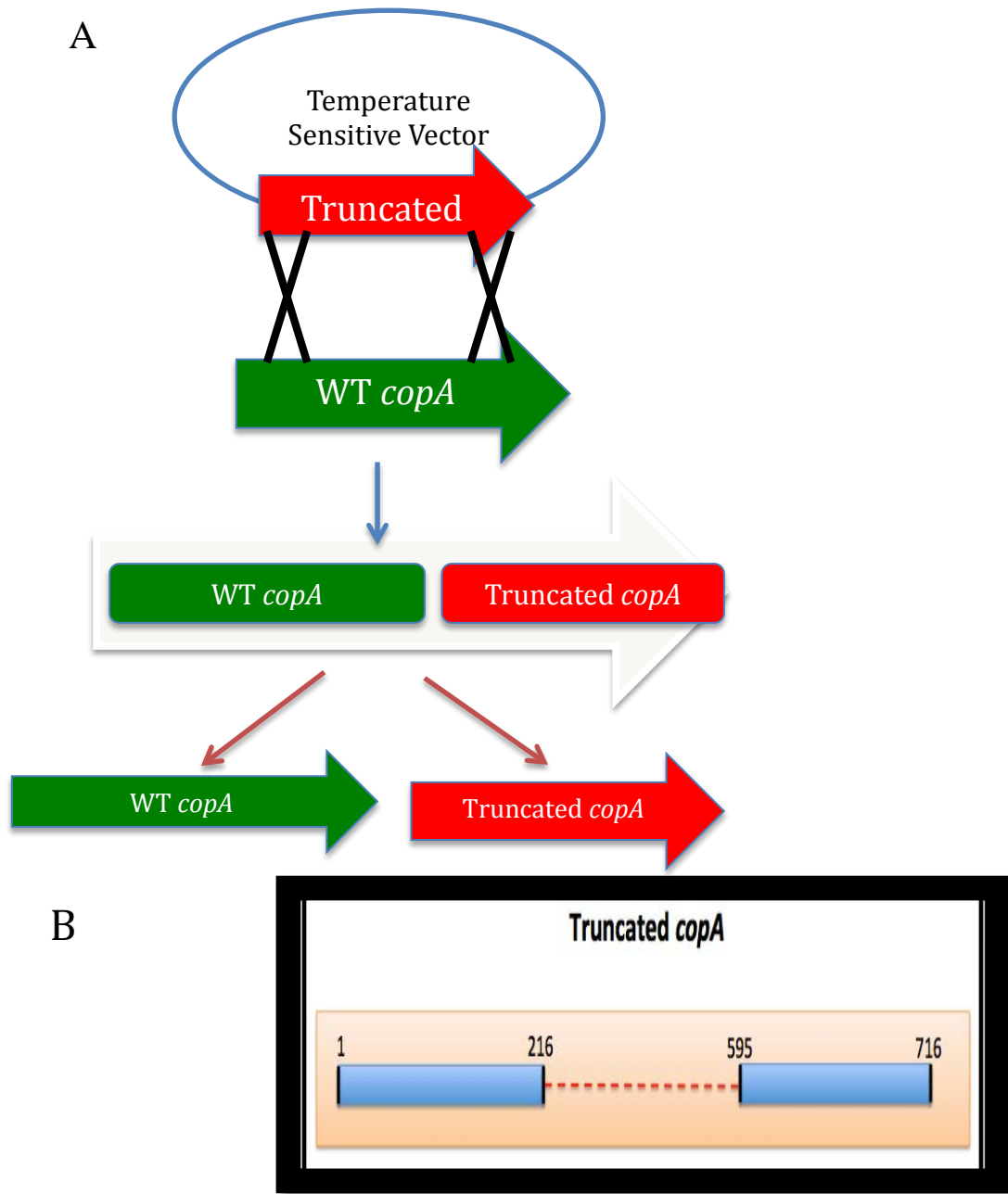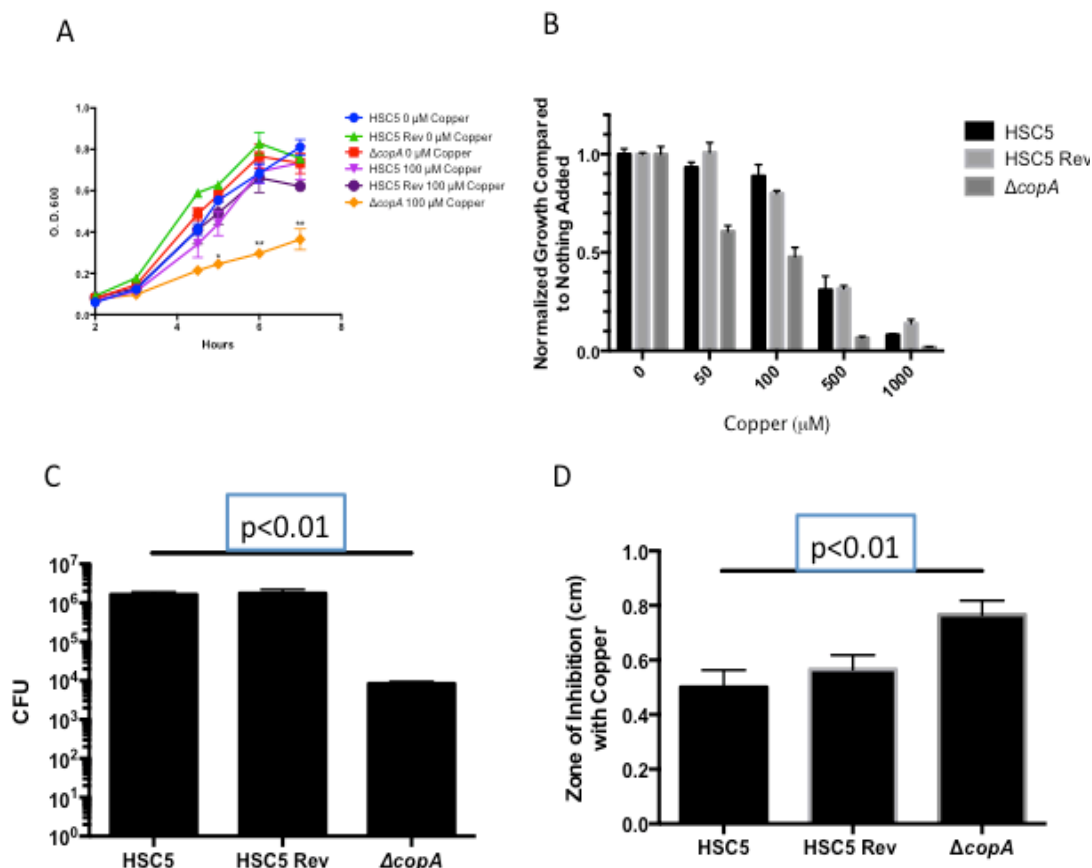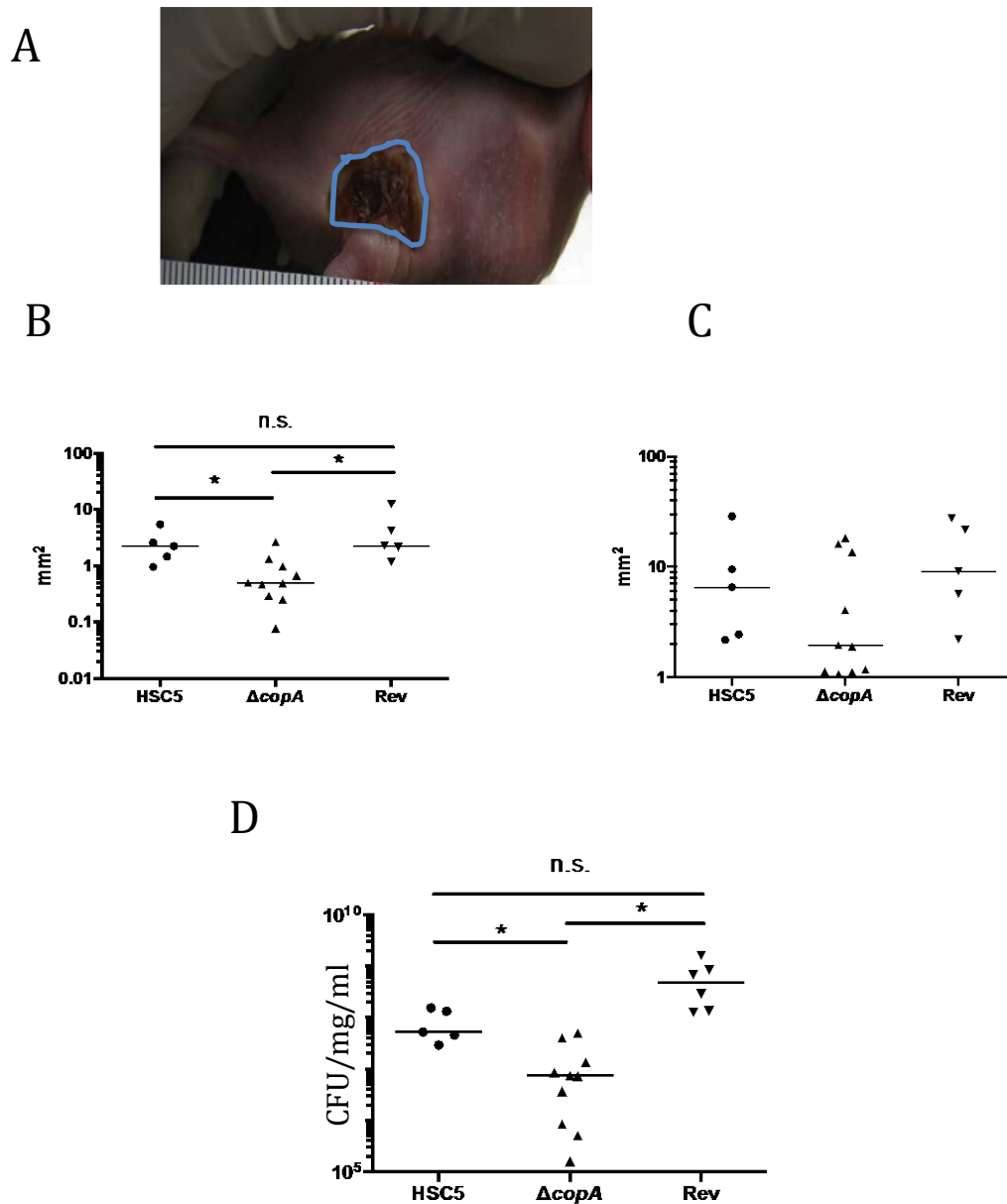
Figure 3

Figure 3. **A. Generation of *copA* knockout via in-frame deletion**. **B. Truncated *copA*.** The gene sequence between 216 and 595 was truncated from the full-length *copA* containing 716 nucleotides.

Figure 4

Figure 4. **Phenotypic characterization of Δ*copA in vitro***
A. *S. pyogenes* **copper toxicity growth curve**. Strains were grown in ThyB (Todd Hewitt Broth) and absorbance values were measured hourly at 600 nm. Error bars represent standard error of experiments performed in triplicate. **B. Growth of HSC5, HSC5 Revertant, and the Δ*copA* mutant at stationary phase**. Strains were grown in ThyB and absorbance values were measured at 600 nm after overnight growth and normalized to growth without copper. Error bars represent standard error of experiments performed in triplicate. **C. CFU from the copper toxicity growth curve D.** *S. pyogenes* **colony forming units (CFU) under copper toxicity.** *S. pyogenes* growing with 50 μM copper after 7 hours was collected, serial diluted, and plated for colony forming units following overnight incubation. Error bars represent standard error. **E.** *S. pyogenes* **anaerobic zone of inhibition**. A small filter paper disc absorbed with 10 µL 1M copper was placed in the middle of each plate containing 100 µL of culture at OD 0.2. Bacteria were grown anaerobically in a gas-pak jar for 12 hours. Zone of inhibition was measured as the distance from the edge of the disc to the border where bacteria grew. Error bars represent standard error.

Figure 5

A

B

C

D

Figure 5. **Virulence of the Δ*copA* mutant**
A. Measuring area of lesions post-subcutaneous infection using free-hand drawing tool in ImageJ. **B. Comparison of lesion areas caused by the wild-type HSC5 and Δ*copA* 24-hour post-infection and C. 48-hour post-infection.** *p-value < 0.05 is calculated using Mann-Whitney U test. **D. CFU of HSC5, the Δ*copA* mutant, and the revertant per mouse were determined 48-hour post-infection.** Bacteria were collected from homogenates of infected lesions and plated on ThyB agar at 37°C for 12 hours.

Figure 6

A

B
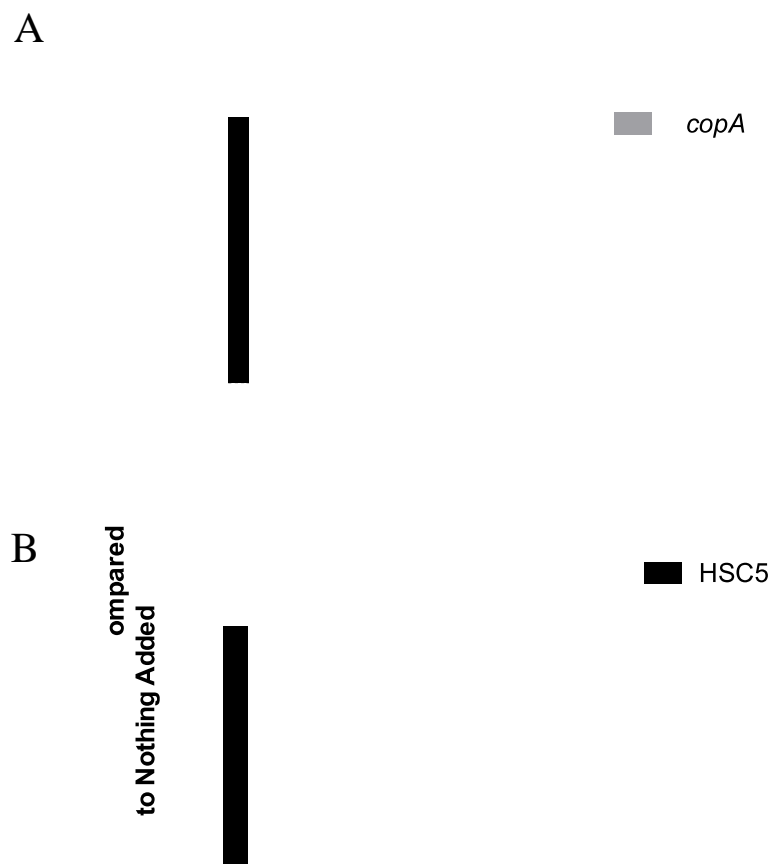
Figure 6. **Increased sensitivity to copper toxicity under anaerobic conditions A. Aerobic growth of HSC5 and the Δ*copA* mutant under copper toxicity.** HSC5 and the Δ*copA* mutant were grown aerobically with varying concentrations of copper. Bacterial growth was measured as OD at 600 nm and normalized to gro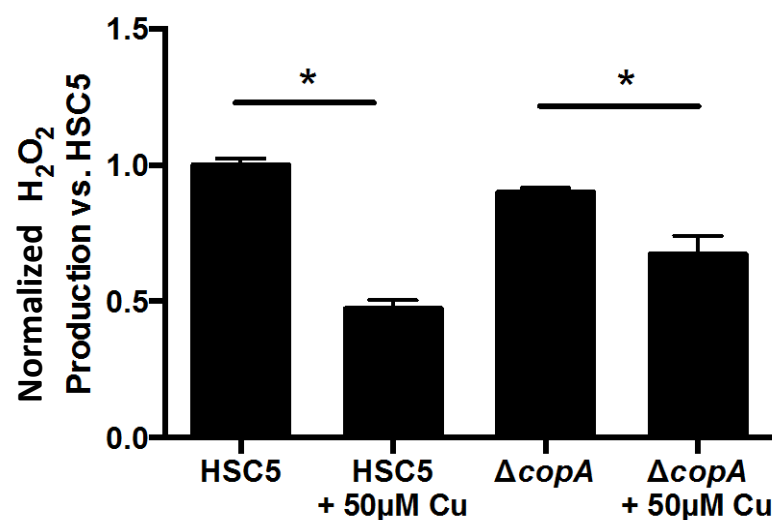wth without copper. Error bars represent standard error. **B. Anaerobic growth of HSC5 and the Δ*copA* mutant with and without copper toxicity.** Anaerobic environment was simulated by oxyrase 20 µL/mL. Bacterial growth was measured as OD at 600 nm and normalized to growth with neither copper nor oxyrase. Error bars represent standard error.

Figure 7

A
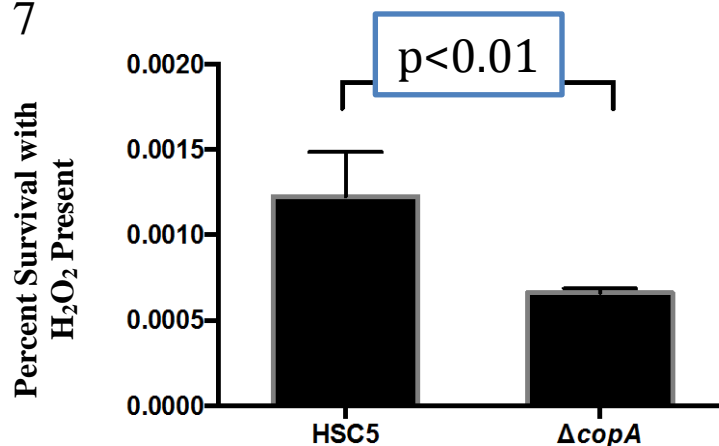
B

Figure 7. **The $\Delta copA$ mutant's sensitivity to H_2O_2 and H_2O_2 production A. Wild-type *S. pyogenes* and the $\Delta copA$ mutant sensitivity under H_2O_2 stress.** Both the wild type HSC5 and $\Delta copA$ at OD 0.4 were exposed to 0.1% final concentrations of H_2O_2 for 30 minutes. Triplicate samples were then serial diluted, plated, and incubated at $37^\circ C$ with 5% CO_2 overnight for determination of CFU. Error bars represent standard error. **B. Wild-type *S. pyogenes* and the $\Delta copA$ mutant H_2O_2 production under copper stress.** Both strains were grown aerobically for 7 hours in ThyB with or without 50 μM copper. Bacterial supernatant was collected for the Amplex Red Hydrogen Peroxide / Peroxidase assay. The fluorescence was measured (excitation at 544 nm and emission detection at 590 nm). Error bars represent standard error. *$p < 0.01$
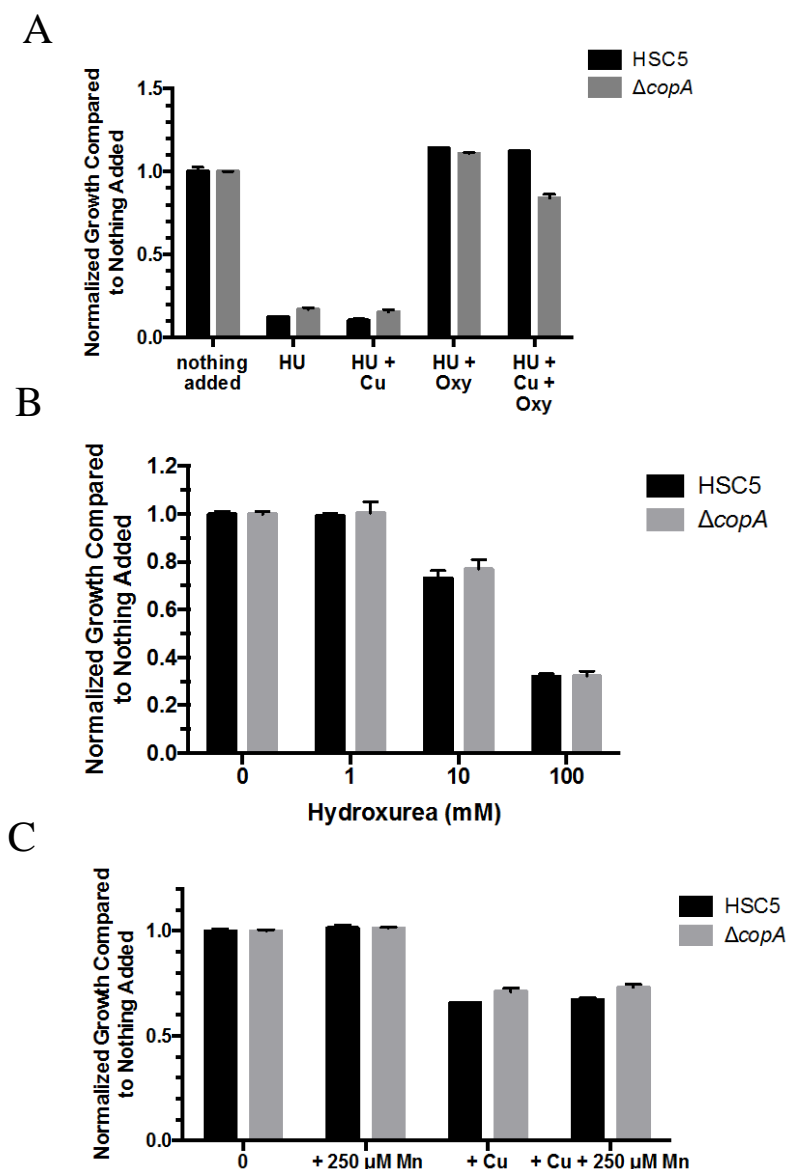
Figure 8

A

B

C

Figure 8. **HSC5 and the Δ*copA* mutant sensitivity to hydroxyurea and Mn^{2+} in the presence of Cu^{2+}**
A. Anaerobic and aerobic growth of HSC5 and the Δ*copA* mutant with hydroxyurea under copper toxicity (HU). HSC5 and the Δ*copA* mutant were grown in 7.5mM HU and/or 50 µM copper and/or 20 µL/mL oxyrase. Bacterial growth was measured as OD at 600 nm and normalized to growth with nothing added. Error bars represent standard error. **B. Growth of HSC5 and the Δ*copA* mutant with varying concentrations of hydroxyurea (HU).** Bacterial growth was measured as OD at 600 nm and normalized to growth with nothing added. Error bars represent standard error. **C. Growth of HSC5 and the Δ*copA* mutant with manganese after 7 hours.** HSC5 and the Δ*copA* mutant were grown in 250 µM Mn^{2+}. Bacterial growth was measured as OD at 600 nm and normalized to growth with neither copper nor manganese. Error bars represent standard error.

Table 1. **RNA Microarray Analysis**. HSC5 and the Δ*copA* mutant were treated with or without 100 µM Cu^{2+} before extraction of RNA with RiboPure RNA Purification Kit.

	Locus tag	Name	Function	Normalized expression
Up regulated	SPy0845	czcD	putative cation-efflux system membrane protein	3.9485
	SPy1714	**copZ**	**putative copper chaperone - copper transport**	**4.635**
	SPy1715	**copA**	**putative cation-transporting ATP-ase - copper**	**5.2775**
	SPy1717	**copY**	**putative negative transcriptional regulator -**	**3.568**
	SPy2039	**speB**	**pyrogenic exotoxin B**	**2.483**
	SPy2110	nrdD	putative anaerobic ribonucleoside-triphosphate	1.2535
	SPy2162	cadD	putative cadmium resistance protein	3.458
	SPy2163	cadC	putative cadmium efflux system accessory	3.227
Down regulated	**SPy0323**	**braB**	**putative branched-chain amino acid transport**	**-1.6065**
	SPy1316	**null**	**putative ABC transporter (ATP-binding protein)**	**-1.973**
	SPy1434	**null**	**putative heavy metal-transporting ATPase**	**-1.742**

Bold text indicates comparison between HSC5+Cu^{2+} and HSC5. Normal text indicates comparison between the Δ*copA* mutant and HSC5.
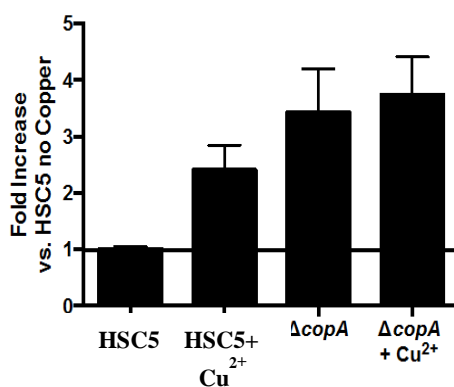
Figure 9

Figure 9. **Real-time PCR confirming the upregulation of *czcD* (S*Py_0845*) under Cu^{2+} stress.** Data were normalized by the expression of HSC5 without Cu^{2+}. Error bars represent standard error.
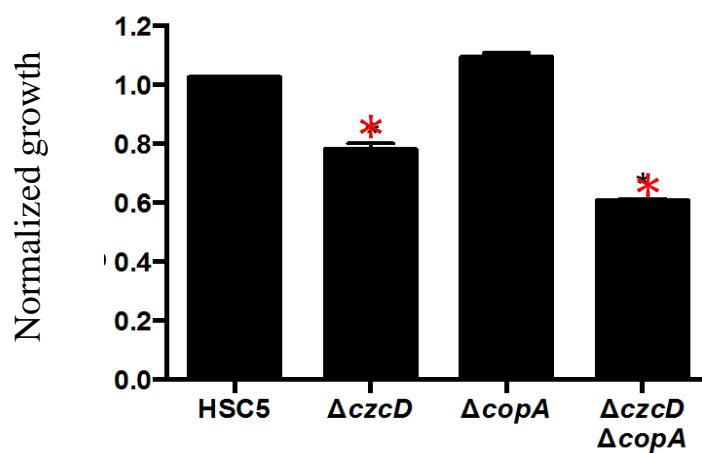
Figure 10

Figure 10. **HSC5, Δ*czcD*, Δ*copA,* and Δ*czcD*Δ*copA* growth under Zn^{2+} stress.** Strains were grown in ThyB pH 6.5 containing 500 μM Zn^{2+}. Absorbance values were measured at 600 nm after overnight growth and normalized to growth without Zn^{2+}. Error bars represent standard error of experiments performed in triplicate.
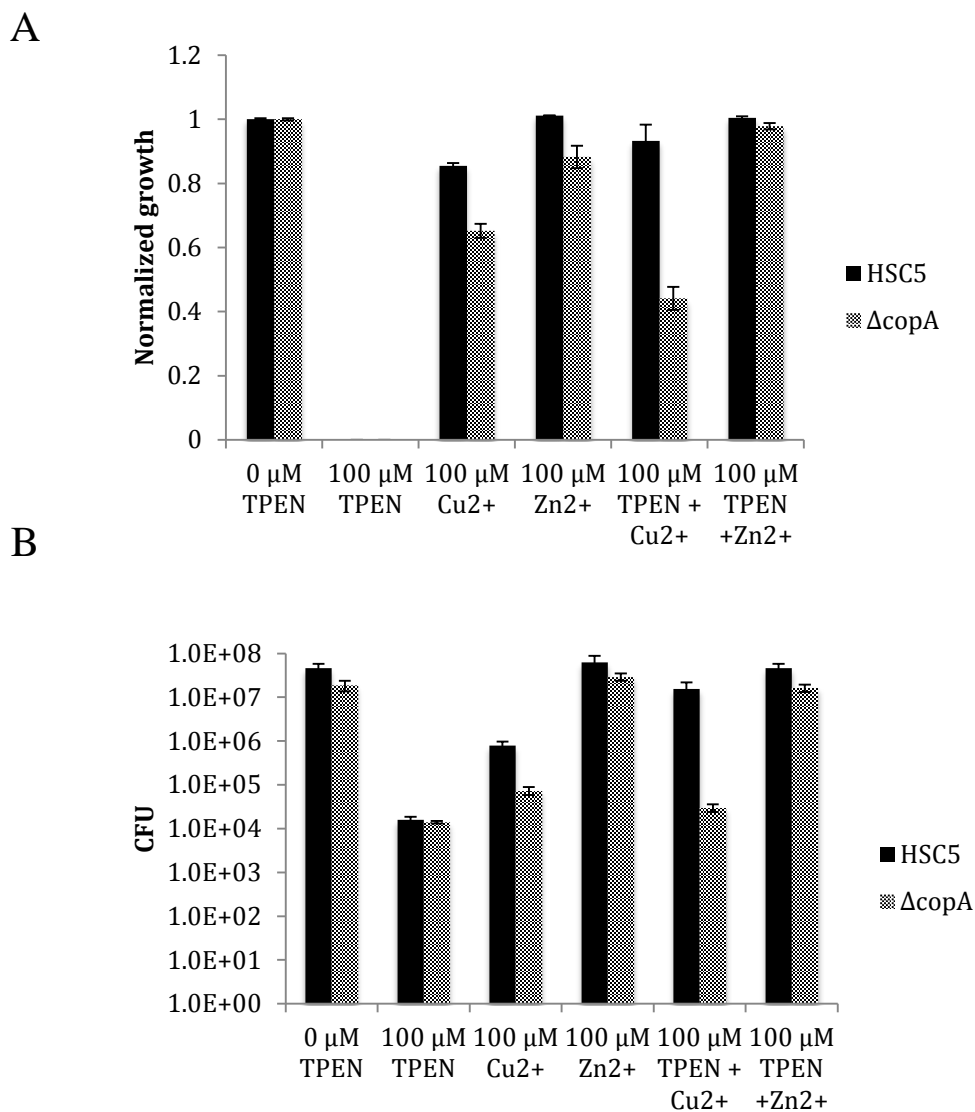
Figure 11

A

B

Figure 11. **Effects of zinc chelation and copper stress**
A. Growth of HSC5 and Δ*copA* under Zn^{2+} chelation and/or Cu^{2+} stress.
Strains were grown in ThyB in TPEN and/or Cu^{2+} and absorbance values
were measured at 600 nm after 24 hours. Data were normalized to growth
without TPEN or Cu^{2+}. **B. *S. pyogenes* CFU from the growth assay.** CFU
counts were determined after *S. pyogenes* was plated on ThyB agar. Error
bars represent standard error of experiments performed in triplicate.
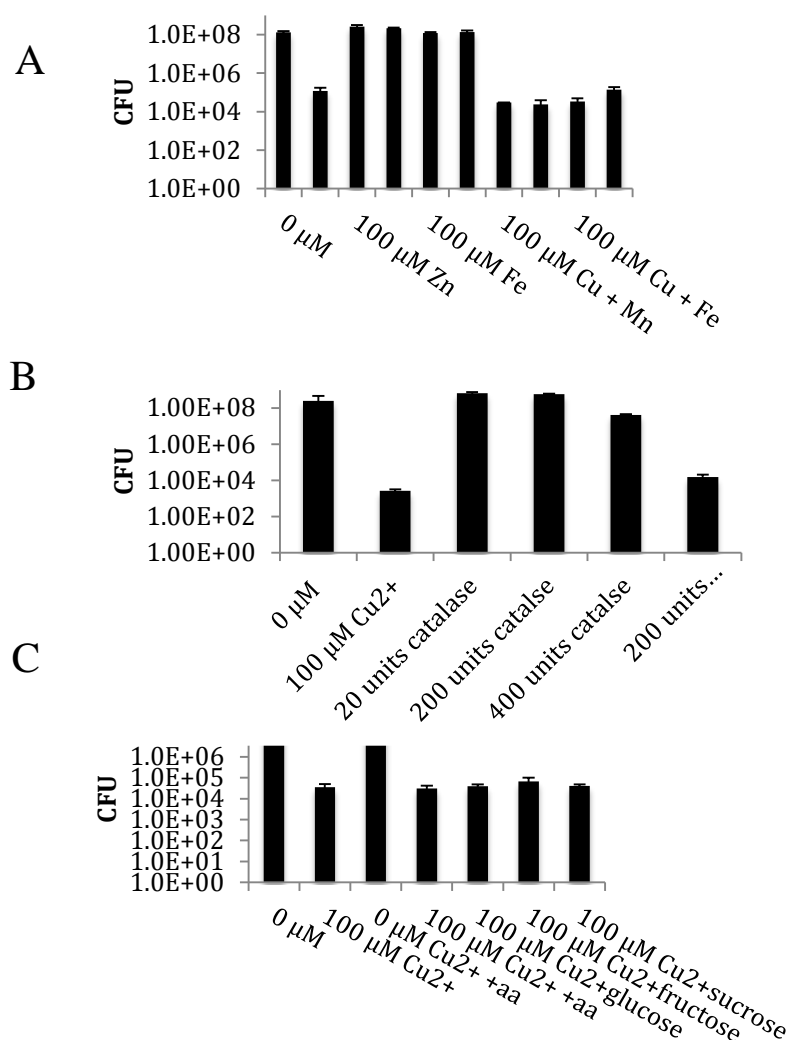
Figure 12

Figure 12. **Effects of divalent cations, catalase, essential amino acids, or carbohydrates on increased copper toxicity during stationary phase A. HSC5 CFUs after growing with divalent cations in addition to Cu^{2+}.** HSC5 was grown in ThyB pH 6.5 containing 100 μM Zn^{2+}, Mn^{2+}, Fe^{2+}, or Mg^{2+} with or without 100 μM Cu^{2+} for 24 hours and plated on ThyB agar. **B. HSC5 CFUs after growing with catalase in addition to Cu^{2+}.** HSC5 was grown in ThyB pH 6.5 containing 100 μM Zn^{2+}, Mn^{2+}, Fe^{2+}, or Mg^{2+} with or without 100 μM Cu^{2+} for 24 hours and plated on ThyB agar. **C. HSC5 CFUs after growing in with essential amino acids in addition to 100 μM Cu^{2+}.** HSC5 was grown in ThyB pH 6.5 supplemented with casamino acids and tryptophan in addition to 100 μM Cu^{2+}. Error bars represent standard deviation.

Figure 13

A

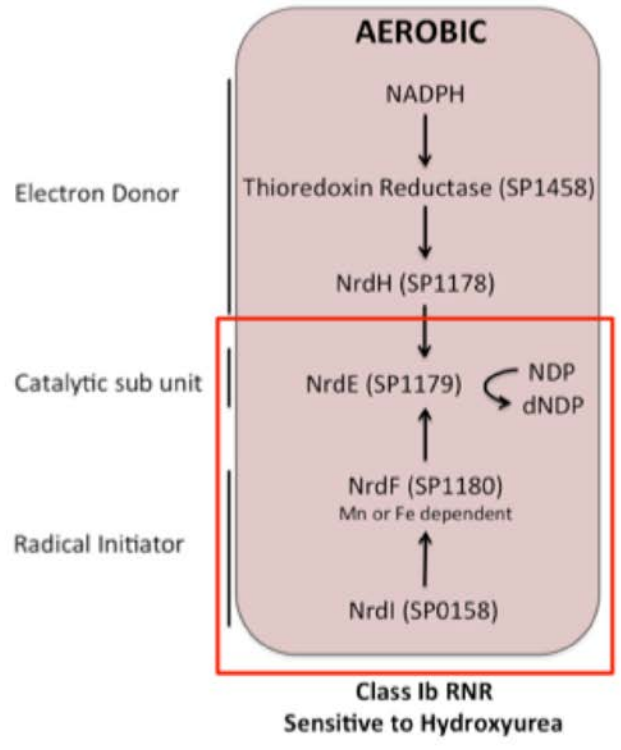| S. pneumoniae	S. pyogenes
ΔcopA is more sensitive to HU than WT	WT and ΔcopA equally sensitive to HU
Mn Rescue – YES Fe Rescue – NO	**Mn Rescue – NO** Fe Rescue – NO

B

Figure 13. **Redundant aerobic dNTP synthesis pathway in** *S. pyogenes* **A. Comparison between** *S. pneumoniae* **and** *S. pyogenes.* **B. Redundant aerobic dNTP synthesis pathway in** *S. pyogenes.* Red box highlights proteins that are duplicated.
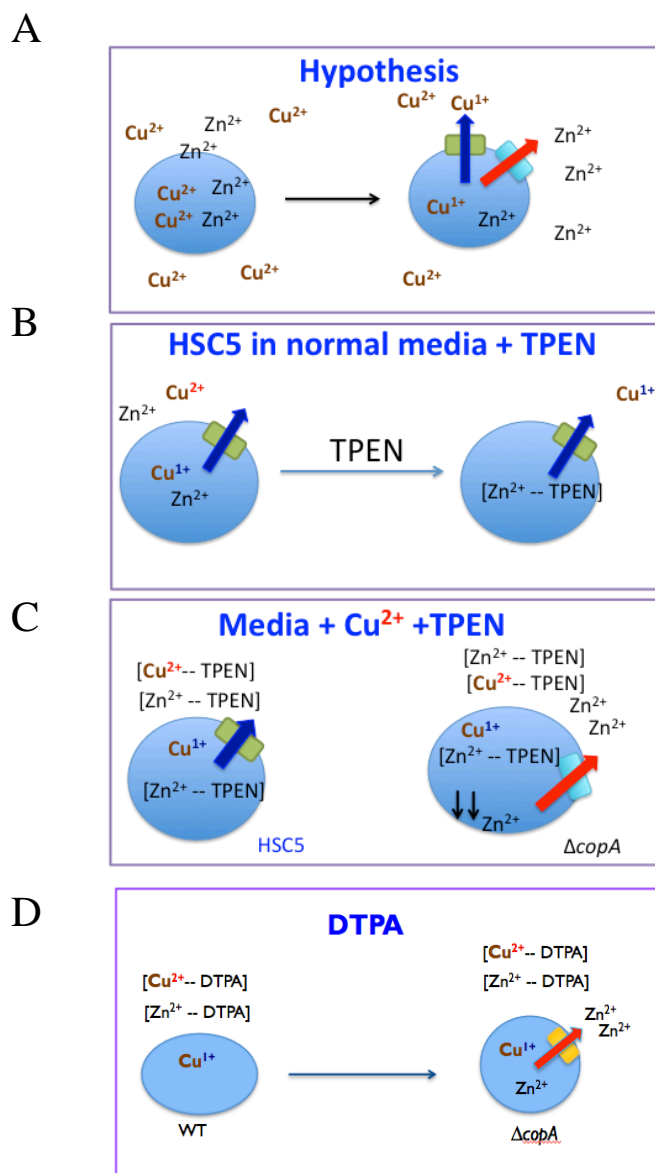
Figure 14

A

B

C

D

Figure 14. **Diagram of effects of zinc chelation by TPEN and DTPA.** Circles represent *S. pyogenes* cells. Blue arrow represents CopA (copper exporter), and red arrow represents CzcD (zinc exporter).
A. Hypothesis. Copper stress induces inappropriate zinc efflux. B**. Effect of TPEN on HSC5.** Cu^{2+} is reduced to Cu^{1+} and then exported by CopA. TPEN chelates intracellular Zn^{2+}. **C. Comparison of TPEN effects on HSC5 and Δ*copA*.** In HSC5, TPEN chelates extracellular Cu^{2+} and Zn^{2+} not intracellular Cu^{1+}. However, wild-type CopA can export Cu^{1+}. In Δ*copA*, the mutated CopA cannot remove excess Cu^{1+}, which becomes toxic. **D. Comparison of DTPA effects on HSC5 and Δ*copA*.** DTPA chelates only extracellular Zn^{2+} and Cu^{2+}. Intracellular Zn^{2+} concentration is not expected to be depleted.

LITERATURE CITED

Carapetis JR, Steer AC, Mulholland EK, and Weber M. 2005. The global burden of group A streptococcal diseases. *The Lancet Infectious Diseases.* 5(11):685-94.

Group A Streptococcal (GAS) Disease. Centers for Disease Control and Prevention. 2008.

Cho YE, Lomeda RR, Ryu SH, Lee JH, Beattie JH, and Kwun IS. 2007. Cellular Zn depletion by metal ion chelators (TPEN, DTPA, and chelex resin) and its application to osteoplastic MC3T3-E1 cells. *Nutri Res Pract.* 1(1): 29-35.

Festa RA and Thiele DJ. 2012. Copper at the Front Line of the Host-Pathogen Battle. *PLoS Pathog.* 8(9): e1002887. doi:10.1371/journal.ppat.1002887.

Huyn HJ, Sohn JH, Ha DW, Ahn YH, Koh JY, and Yoon YH. 2001. Depletion of intracellular zinc and copper with TPEN results in apoptosis of cultured human retinal pigment epithelial cells. *Invest. Ophthalmol. Vis. Sci.* 42(2):460-465.

Johnson MD, Kehl-Fie TE, and Rosch JW. 2015. Copper intoxication inhibits aerobic nucleotide synthesis in *Streptococcus pneumoniae. Metallomics.* doi: 10.1039/C5MT00011D.

Johnson MD, Kehl-Fie TE, Klein R, Kelly J, Burnham C, Mann B, and Rosch JW. 2015. Role of copper efflux in pneumococcal pathogenesis and resistance to macrophage-mediated immune clearance. *Infect Immun.* 83(4):1684-94.

Martin JE and Imlay JA. 2011. The alternative aerobic ribonucleotide reductase of *Escherichia coli*, NrdEF, is a manganese-dependent enzyme that enables cell replication during periods of iron starvation. *Molecular Microbiology.* 80:319-334.

Macomber L and Imlay JA. 2009. The iron-sulfur clusters of dehydratases are primary intracellular targets of copper toxicity. *Proc Natil Acad Sci USA.* 106(20):8344-8339.

McBrien DC. 1980. Anaerobic potentiation of copper toxicity and some environmental considerations. *Ciba Foundation Symposium.* 79:301-18.

Mu D, Lopez MM, Masuda Y, and Kuipers OP. 2013. Zirex: a novel zinc-regulated expression system for *Lactococcus lactis. Appl. Environ. Microbiol.* 79(14): 4503-4508.

Ogawa T, Terao Y, Sakata H, Okuni H, Ninomiya K, Ikebe K, Maeda Y and Kawabata S. 2011. Epidemiological characterization of *Streptococcus pyogenes* isolated from patients with multiple onsets of pharyngitis. *FEMS Microbiology Letters*, 318:143-151.

Palm-Espling ME, Niemiec MS, Wittung-Stafshede P. 2012. Role of metal in folding and stability of copper proteins *in vitro. Molecular Cell Research,* 1823:1594-1603.

Ricci S*,* Janulczyk R, and Björck L. 2002. The regulator PerR is involved in oxidative stress reponse and iron homeostasis and is necessary for full virulence of *Streptococcus pyogenes.* 70(9):4968-4976.

Seki M, Iida K, Saito M, Nakayama H, and Yoshida S. 2004. Hydrogren peroxide production in *Streptococcus pygones:* Involvement of lactate oxidase and coupling with aerobic utilization of lactate. *Journal of Bacteriology*. 186:2046-2051.

Wiggs L, Cavallaro J, and Miller M. 2000. Evaluation of oxyrase OxyPlate anaerobe incubation system. *Journal of Clinical Microbiology,* 38:499-507.

Yarbro JW. 1992. Mechanism of action of hydroxyurea. *Seminars in Oncology,* 3:1-10.